APPENDIX 10A

PREDICTION OF REGIONAL DEPOSITION IN THE HUMAN RESPIRATORY TRACT USING THE INTERNATIONAL COMMISSION ON RADIOLOGICAL PROTECTION PUBLICATION 66 MODEL

10A.1 INTRODUCTION

This Appendix gives an overview of how the regional deposition values that are calculated using the ICRP's newly recommended model of the human respiratory tract (ICRP66, 1994) compare with the available body of experimental data. A more complete description and discussion of these data is given in Annexe D (James et al., 1994) of the ICRP66 report. That Annexe also discusses both the theoretical model (Egan et al., 1989) of gas and aerosol particle transport in the human respiratory tract, which underlies ICRP66's analysis of the experimental data, and ICRP66's methodology in developing the recommended algebraic expressions to predict regional deposition for various subjects.

The deposition of particles in the respiratory tract, and the underlying physical mechanisms that determine regional deposition, have been intensively studied. However, in the main, experimental data are available only for the adult Caucasian male, and for a limited range of particle size (from about 1-μm to 10-μm aerodynamic diameter), whereas the application of this human respiratory tract model is required to be much broader. Because of the need to extrapolate the available data to aerosol particles and vapors from atomic dimensions up to very coarse wind-borne particles, and also to subjects of different body size and level of physical exertion, the ICRP66 report applied both theoretical and/or empirical modeling methods, as appropriate, to develop the recommended predictive deposition model.

Since the publication of ICRP's previous deposition model (TGLD, 1966; ICRP, 1979), substantial progress has been made in theoretical modeling of aerosol transport and deposition within the lungs (Taulbee and Yu, 1975; Pack et al., 1977; Yu, 1978; Nixon and Egan, 1987). The development of this theoretical modeling approach was reviewed by Heyder and Rudolf (1984). As a working hypothesis, the ICRP66 report utilized the particular formulation described by Egan and Nixon (1985), and later improved by Egan et al. (1989), as the basis for modeling regional aerosol deposition in the lungs of different subjects as a function of their respiratory characteristics.

In parallel with this more fundamental approach to modeling in purely physical terms, substantial developments have occurred in the analysis of measured particle deposition in the respiratory tract in terms of empirically defined parameters (TGLD, 1966; Davies, 1972; Rudolf et al., 1986, 1990). As a working hypothesis, the ICRP66 report utilized the parametric analysis of regional lung deposition developed by Rudolf et al. (1990) to represent the results of complex

theoretical modeling by relatively simple algebraic approximations. The algebraic formulae so developed and described in the Annexe to ICRP66 constitute ICRP's recommended respiratory tract deposition model.

In ICRP66, and in this annex, the term "deposition" denotes the mean probability of an inspired particle being deposited. The fraction of the number of inhaled particles deposited in the whole respiratory tract is referred to as "total" deposition. The fraction of the number of inhaled particles deposited in a single region of the respiratory tract is referred to as "regional" deposition. The total deposition is therefore the sum of the regional deposition values. The term "deposition efficiency" denotes the fraction of the number of particles that enter a single region of the respiratory tract that is deposited in that region.

10A.2 EXTRATHORACIC DEPOSITION

The processes that govern deposition of particles in the extrathoracic region of the respiratory tract, i.e., the nose, naso-oropharyngeal passages, and larynx, depend strongly on particle size (as they do within the thoracic airways). In broad terms, particles with an aerodynamic diameter larger than about 0.5 μm are deposited primarily by the so-called "aerodynamic" transport processes of inertial motion, referred to as "impaction," and gravitational settling, referred to as "sedimentation." For very large particles and fibers, interception with surfaces in the extrathoracic airways also contributes to their deposition. Particles with an equivalent physical diameter less than a few tenths of a micrometer are deposited primarily by the "thermodynamic" transport process of Brownian "diffusion."

10A.2.1 Nasal Deposition

The aerodynamic filtration efficiency of the nose is much better documented than that of any other part of the respiratory tract. A large number of studies have been reported for aerosols with aerodynamic particle diameters above 0.2 μm. These studies have been reviewed by Mercer (1975), Lippmann (1977), Yu et al. (1981), Schlesinger (1985a), and Stahlhofen et al. (1989). As discussed in Annexe D of ICRP66, different experimental techniques and evaluation procedures were used in the various studies, and the published data are not all directly comparable. The artificial technique of measuring nasal deposition when aerosol particles were drawn in continuously through the nose and exhausted through a filter at the mouth gave

generally lower values than other techniques which utilized normal breathing. Accordingly, ICRP66 fitted the recommended empirical model of nasal deposition efficiency to the experimental data obtained with normal breathing.

Figure 10A-1 shows the experimental data on the aerodynamic deposition efficiency of the nose during normal inspiration, plotted as a function of the inertial impaction parameter, $d_{ae}^2 \dot{V}$, where d_{ae} is the aerodynamic particle diameter (in μm), and $\dot{V}$ is the volumetric flow rate (in $cm^3 s^{-1}$). Each of the studies by Lippmann (1970), Giacomelli-Maltoni et al. (1972), and Rudolf (1975) exhibit a large degree of variability in nasal deposition measured in different subjects.

ICRP66 adopted the empirical analysis reported by Rudolf et al. (1986) and Stahlhofen et al. (1989) to represent the trend of the mean of these data for aerodynamic deposition efficiency of the nose on inhalation in terms of the impaction parameter, $d_{ae}^2 \dot{V}$. The recommended function is shown in Figure 10A-1(a), together with the estimated 95% confidence bounds based on the variability of the data. The fitted function accounts for the observed slow increase in deposition efficiency for low values of $d_{ae}^2 \dot{V}$, and also predicts an asymptotic approach to unity for high values of this impaction parameter. As shown in the figure, for intermediate values of $d_{ae}^2 \dot{V}$, the predicted deposition efficiency is similar to that given by Pattle's (1961) log-linear approximation, which was adopted by the Task Group on Lung Dynamics (TGLD, 1966).

Nasal deposition for submicron-sized particles has not been studied intensively in human subjects. Accordingly, to define the "thermodynamic" deposition efficiency of the nose, ICRP66 relied on the experimental measurements made in hollow, anatomical casts of the nasal airways (Swift et al., 1992). (See ICRP66 Annexe D for discussion of these data, and their empirical representation).

10A.2.2 Oropharyngeal Deposition

Most experimental studies of oropharyngeal deposition have been performed with mouth breathing through a tube, since this is a convenient method for aerosol administration. The oral deposition was measured by repeated mouth-washings directly after inhalation. The remainder of the extrathoracic deposition, i.e., that in the oropharynx and larynx, was measured by external gamma counting. Emmett and Aitken (1982) showed that, for particles

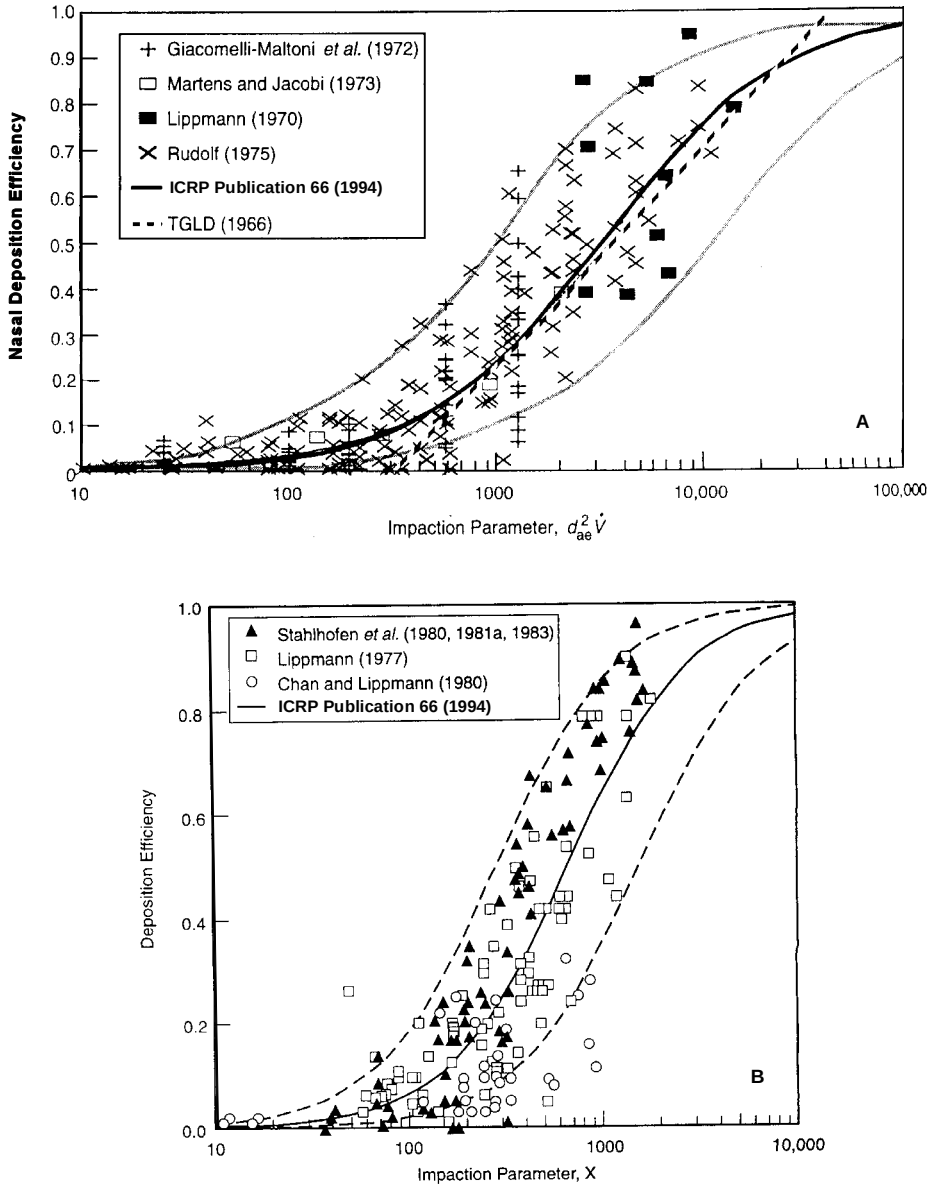

Figure 10A-1. Nasal deposition efficiency measured in adult Caucasian males during normal breathing (A) and data on extrathoracic deposition when particles are inhaled and exhaled through a mouthpiece (B). The solid curves show the empirical model used in ICRP Publication 66 (1994). The outer curves on either side represent the estimated 95% confidence bounds in predicted extrathoracic deposition based on the variability of the data. The heavy dashed line in (A) shows the expression for nasal deposition efficiency used in the ICRP Publication 30 (1979) lung model (TGLD, 1966). The impaction parameter, x, is described in the text as $d_{ae}^2 \dot{V}^{0.6} V_T^{-0.2}$ (μm^2 $cm^{1.2}$ $s^{0.6}$).

Source: ICRP Publication 66 (1994).

less than about 10-μm aerodynamic diameter, the bulk of the extrathoracic deposition during mouth breathing occurs in the larynx.

Figure 10A-1(b) compares the experimental data on extrathoracic deposition during mouth breathing through tube mouthpieces obtained by Lippmann (1977), Chan and Lippmann (1980), and Stahlhofen et al. (1980, 1981a, 1983). Again, the measured variability in extrathoracic deposition is high. The curves shown in the figure represent the empirical model adopted in ICRP66 to describe the underlying trend of deposition efficiency as a function of an impaction parameter, (see also Figure 10-22 of Chapter 10), together with the upper and lower 95% confidence bounds of this estimate.

10A.2.3 Scaling for Body Size

Extrathoracic deposition has not been studied systematically in children, nor has the degree to which the intersubject variability measured in adult subjects is related to variation in anatomical dimensions. In the absence of data, ICRP66 utilized the dimensional scaling procedure proposed by Swift (1989) to predict the effect of a subject's body size on nasal and oropharyngeal deposition of particles in the aerodynamic size-range, and by Cheng et al. (1988) to predict body-size effects on thermodynamic deposition efficiency, in relation to values modeled for a reference adult male.

10A.3 REGIONAL LUNG DEPOSITION

Although the experimental data obtained for the adult human male are sufficient to model empirically and accurately the deposition efficiency of the lungs as a whole, as a function of breathing behavior and particle size (Rudolf et al., 1983, 1986), they are not complete enough nor mutually consistent enough to define precisely the regional deposition in a reference adult male, nor the effects of different airway size in other subjects. ICRP66 therefore used the theoretical model developed by Egan and Nixon (1985), and Nixon and Egan (1987), as updated by Egan et al. (1989), to predict the effects of breathing behavior and airway size on the deposition of particles in discrete anatomical regions of the lungs, i.e., in the bronchial (BB), bronchiolar (bb), and alveolar-interstitial (AI) airways, of various subjects. These theoretical predictions formed the basis for the simplified algebraic model of regional deposition in the

lungs of various subjects that is recommended in ICRP66, and is applied in Chapter 10. The model evaluates the combined effects of convective and diffusive gas transport, and aerosol loss processes, within the airways of the lungs, on the basis of the mathematical formalisms introduced by Taulbee and Yu (1975) and Pack et al. (1977).

10A.3.1 Comparison with Data from GSF Frankfurt Laboratory

Stahlhofen et al. (1980, 1981a,b, 1983) measured the fractional deposition of insoluble monodisperse aerosols of iron oxide particles labeled with ^{198}Au, in a total of nine different subjects under closely controlled breathing conditions. In these tests, the subjects inhaled and exhaled particles of various sizes through a mouthpiece, at a constant flow rate of either 250 cm^3 s^{-1} or 750 cm^3 s^{-1}. Four different tidal volumes were studied: 250 cm^3, 500 cm^3, 1000 cm^3 at the flow rate of 250 cm^3 s^{-1}, and 1500 cm^3 at the flow rate of 750 cm^3 s^{-1}. The fraction of inhaled gamma activity deposited initially in the thorax was measured using a calibrated and well-characterized array of collimated NaI(Tl)-detectors. The retention of the deposited iron oxide particles in the lungs (obtained by correcting the thorax measurements for the activity of particles cleared to the stomach) was followed in each subject for several days. In general, two distinct phases of particle retention were observed: an initial rapid phase, succeeded by continued slow clearance with a fitted half-time of several tens of days. The exponential clearance curve fitted to the "slow-cleared" fraction was extrapolated back to the time of exposure to define the complementary "fast-cleared" fraction of the initial lung deposit. The "slow-" and "fast-cleared" fractions of the thoracic deposit are conventionally assumed to represent particles deposited in the A region and tracheobronchiolar airways (BB and bb regions), respectively.

To simulate these experimental data, ICRP66 utilized the theoretical deposition model of Egan et al. (1989) to calculate the expected fractional deposition summed for all airways in the A region and the combined BB and bb regions. Figures 10A-2 and 10A-3 compare the theoretical predictions of tracheobronchiolar and alveolar-interstitial deposition, respectively, with the "fast-" and "slow-cleared" fractions of thoracic deposition measured at the GSF Frankfurt Laboratory.

It is seen from these figures that both measured fractions of the thoracic deposition exhibit substantial variability under otherwise identical experimental conditions (as does the

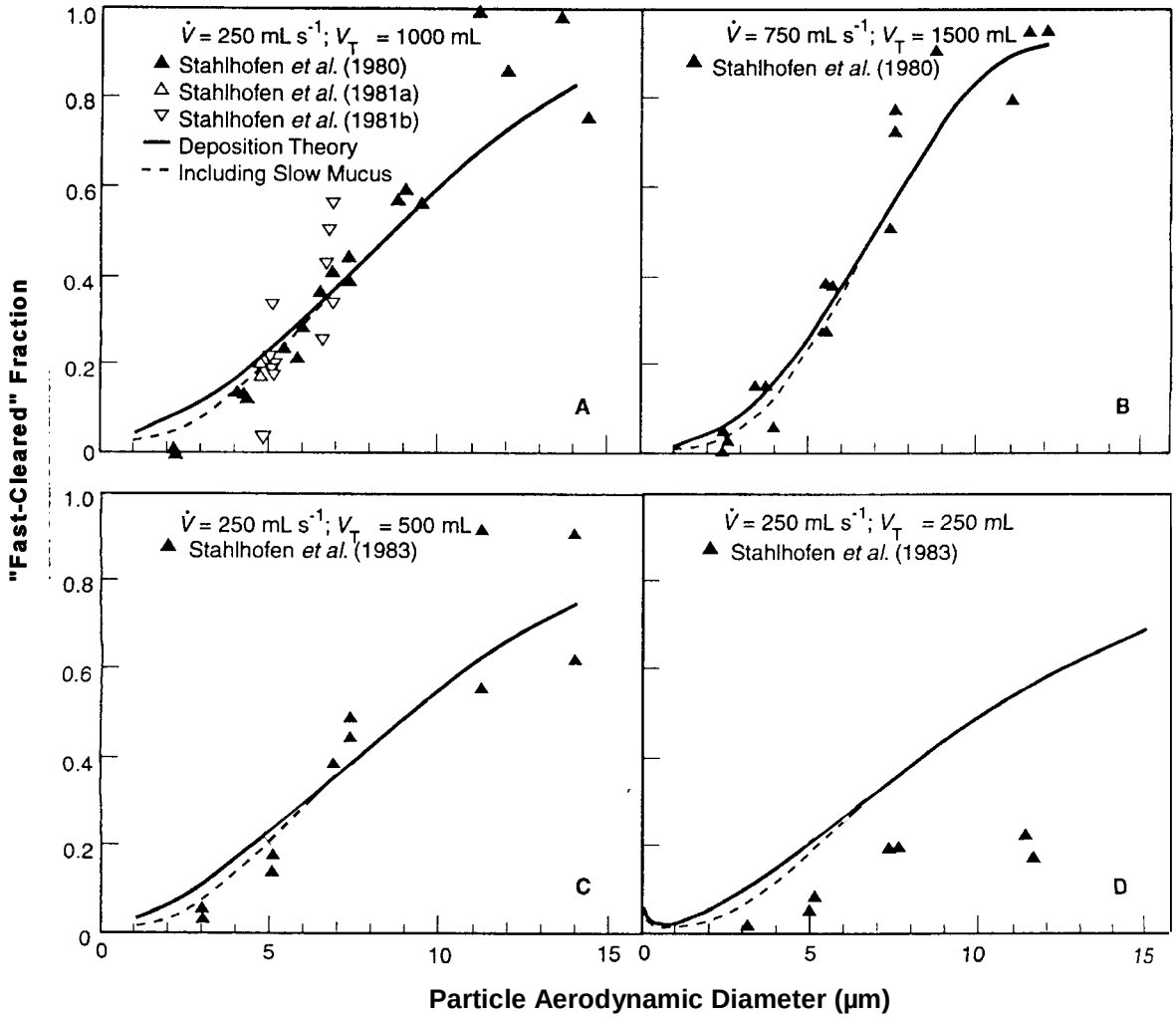

Figure 10A-2. Comparisons of the "fast-cleared" fraction of lung deposition measured at the GSF Frankfurt Laboratory with the tracheobronchiolar deposition predicted by the theoretical model (shown by the solid curves) of Egan et al. (1989). The dashed curves show the effect on the predicted "fast-cleared" fraction of allowing for slow clearance of a fraction of the number of particles deposited in the tracheobronchiolar airways. This "slow-cleared" fraction is assumed to tend to zero for large particles.

Source: ICRP Publication 66 (1994).

total thoracic deposition). It is also seen that, overall, the calculated deposition curves provide an accurate prediction of the trends in measured values with particle aerodynamic diameter.

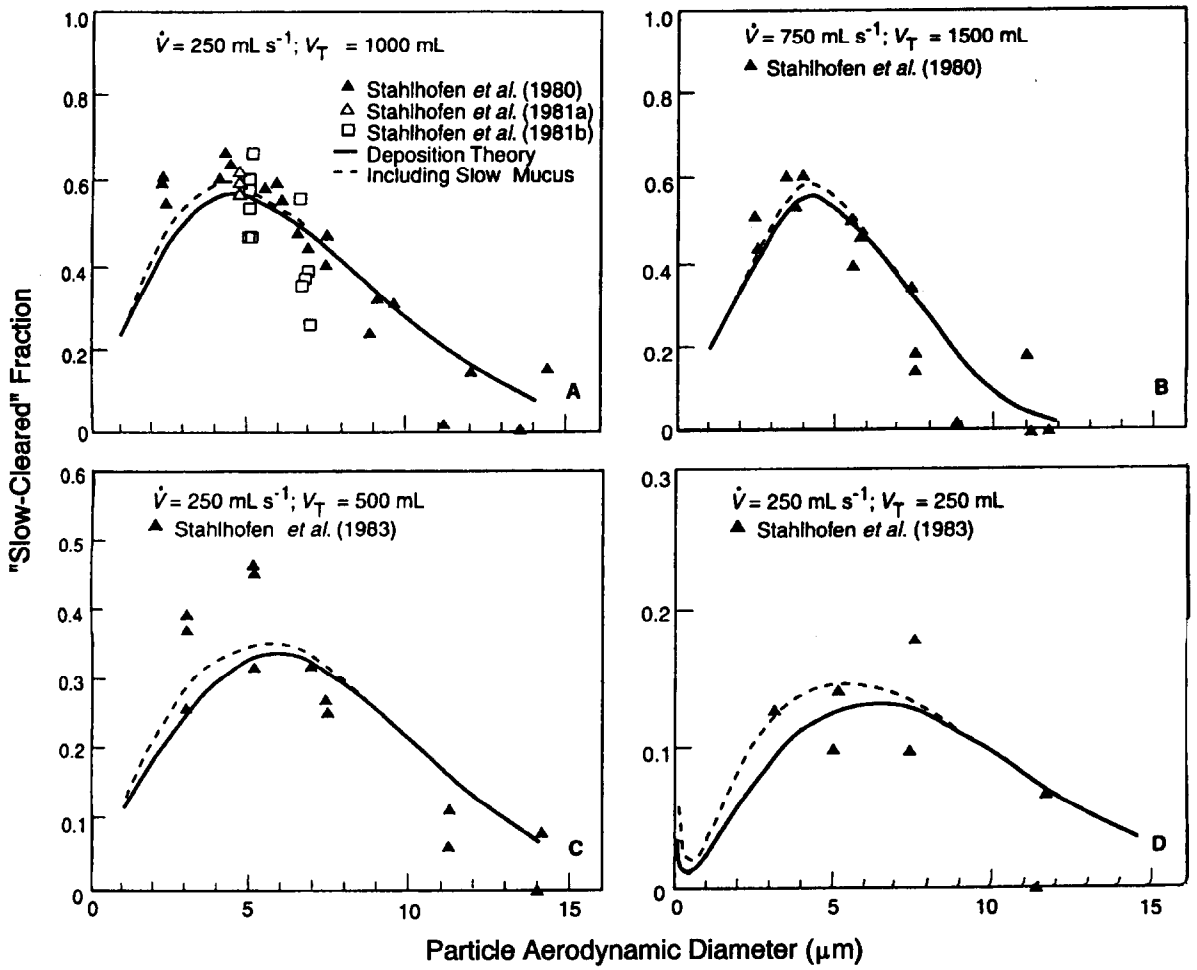

Figure 10A-3. Comparisons of the "slow-cleared" fraction of lung deposition measured at the GSF Frankfurt Laboratory with the alveolar deposition predicted by the theoretical model (shown by the solid curves) of Egan et al. (1989). The dashed curves show the effect on the predicted "slow-cleared" fraction of allowing for additional slow clearance of a fraction of the number of particles deposited in the tracheobronchiolar airways.

Source: ICRP Publication 66 (1994).

In Figure 10A-2, except for the experiments carried out at a flow rate of 250 cm^3 s^{-1} and a low tidal volume of 250 cm^3 (Figure 10A-2(d)), it is seen that the predicted curves match the measured "fast-cleared" fractions. The closest match is obtained for the experiments carried out at a flow rate of 750 cm^3 s^{-1} and tidal volume of 1500 cm^3

approximates the breathing rate of ICRP66's "reference worker." The apparently poor match to the data at low flow rate and low tidal volume arises principally from the two measurements for 12-μm-aerodynamic-diameter particles. Bronchial deposition efficiency for these particles should clearly be substantially higher than for the next smallest particles (of 7.5-μm aerodynamic diameter). The fact that the measured efficiency is lower suggests an experimental artifact in correcting for extrathoracic particle losses.

On the whole, the predicted deposition fractions are seen to match the data with increased accuracy as the particle aerodynamic diameter is increased. For several of the smallest particle sizes studied, there is a general tendency for the predicted tracheobronchial deposition to be higher than the measured "fast-cleared" fraction. However, for these particles (with aerodynamic diameter less than about 5 μm), the fit of the predicted curves to the measured values is significantly improved by allowing for the incomplete "rapid" clearance of particles deposited in the human tracheobronchial tree that has been observed directly in other experimental studies. Those studies were discussed in detail in Annexe E (Bailey and Roy, 1994) of ICRP66. Based on that discussion, ICRP66 concluded that, for particles with a physical diameter of 2.5 μm or less, only 50% of the number deposited in the tracheobronchial airways is cleared rapidly. The remaining 50% is cleared at a rate that is indistinguishable experimentally from particles deposited in the alveolar-interstitial airways. For larger particles, the fraction of the tracheobronchial deposition that is cleared slowly is found to decrease steeply with particle size. The dashed curves shown in Figure 10A-2 make allowance for slow clearance of a part of the tracheobronchial deposition. It is seen that, by making this allowance, the fit of the predicted "fast-cleared" fraction to the measured values is improved.

Figure 10A-3 compares the experimental data and theoretical predictions of the complementary "slow-cleared" fraction of lung deposition. For particles with aerodynamic diameter 5 μm or greater, the fit between predicted and measured values is generally good. Allowance for part of the predicted tracheobronchiolar deposition being cleared slowly is again seen to improve the predictions for smaller particles.

10A.3.2 Comparison with Data for Polystyrene Particles

The GSF Laboratory used a so-called "academic" breathing pattern, in which the subject inhaled and exhaled at a closely controlled rate. Other investigators exposed their subjects under so-called "spontaneous" breathing conditions, where the subject maintains a more natural variation in flow rate through the breathing cycle, but is trained to achieve a relatively constant tidal volume and respiratory frequency. In this manner, Foord et al. (1978) measured the fractional deposition of ^{99m}Tc-labelled polystyrene particles in the mouth and lungs of 15 different subjects. The lung deposition was divided into a "tracheobronchiolar" fraction, which was assumed to consist of the activity cleared from the lungs within 24 h of inhalation, and the remaining "pulmonary" fraction. These authors used three different sizes of particles, i.e., 2.5-μm, 5-μm, and 7.5-μm diameter, and studied regional deposition for several different breathing patterns. Figure 10A-4 shows their results for 6 subjects (with an average tidal volume of 1 L, and a mean respiratory frequency of 10 min^{-1}), together with the deposition of ^{99m}Tc-labelled polystyrene particles in the lungs of 12 different subjects measured by Emmett and Aitken (1982), using the same breathing pattern.

The figure shows that, after correcting for the extrathoracic deposition measured for each test, the recommended lung deposition model accurately matches the trend of tracheobronchiolar "deposition" with particle size measured by Foord et al (1978). (See panel labeled "TB"). The calculated curve here includes ICRP66's recommended allowance for an assumed fraction of 50% the TB deposition of the 2.5-μm particles not being cleared from the TB region within the 24-h measurement period. The tracheobronchiolar deposition reported by Emmett and Aitken (1982), i.e., the activity deposited in the lungs that is cleared within 24 h, is generally higher than that found by Foord et al. (1978), with relatively little variability between the three subjects studied at each particle size.

The panel labeled "A" in Figure 10A-4 shows the measured values of activity deposited in the lungs that was retained longer than 24 h. In this case, the data of Foord et al. are generally higher than the modeled values, while Emmett and Aitken's values are lower by a similar factor. Both sets of data show a similar trend of "slow-cleared" lung deposition with particle size to that modeled, but with higher or lower absolute values, respectively, for the same breathing pattern.

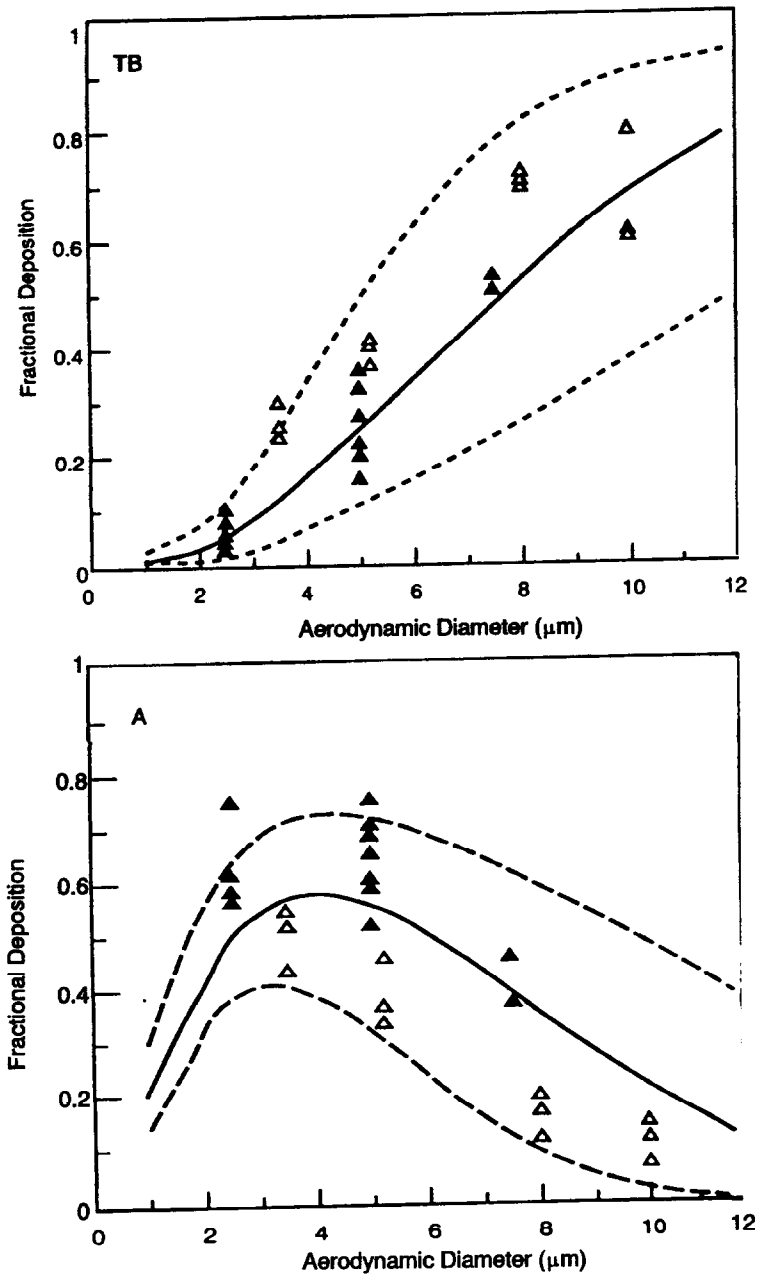

Figure 10A-4. Comparison of fractional deposition measured by Foord et al. (1978) (solid triangles) and Emmett and Aitken (1982) (open triangles) in different subjects with values given by the International Commission on Radiological Protection (ICRP) Publication 66 (1994) lung model (solid curves). The fractional deposition shown has been adjusted to correspond to zero extrathoracic deposition in the tracheobronchial (TB) and alveolar (A) regions. The dashed curves represent the upper and lower 95% confidence bounds of regional deposition predicted for an individual subject by the ICRP lung model.

Source: ICRP Publication 66 (1994).

When the experimental data on thoracic deposition in "fast-" and "slow-cleared" fractions are pooled, as is done in Figure 10A-4, the deposition model recommended in ICRP66 represents the data as a whole. It is also seen from Figure 10A-4 that ICRP66's estimated 95% confidence bounds on regional lung deposition predicted for individual subjects include all but 3 of the data points.

10A.3.3 Comparison with Data for Submicron-Sized Particles

For particles in the submicron, thermodynamic size range (with equivalent diameter between about 5 nm and 0.2 μm), extrathoracic deposition during mouth breathing (in the oral cavity and larynx) is small compared to that in the lungs. Schiller et al. (1986) measured the total respiratory tract deposition for several subjects exposed via a mouthpiece to monodisperse, uncharged spherical particles of silver over a range of particle diameter extending from 5 nm to about 0.2 μm. These experimental results were corrected by Gebhart et al. (1989) for the effects of instrumental dead space, which tended to reduce the measured deposition fraction for nanometer-sized particles. Egan and Nixon (1989) compared the resulting mean values of total thoracic deposition with the values predicted by the theoretical model developed by Egan et al. (1989). These authors showed that the theoretically modeled fractional deposition in the lungs matches the measured values. Figure 10A-5 shows that the calculated values also represent the data obtained earlier for hydrophobic submicron-sized spheres of aluminosilicate by Tu and Knutson (1984).

10A.3.4 Influence of "Controlled" Versus "Spontaneous" Breathing

The data from the GSF Frankfurt Laboratory shown above apply to controlled breathing at a constant inspiratory and expiratory flow rate, whereas, during normal spontaneous breathing, the flow rate varies throughout each breath in an approximately sinusoidal manner. However, Heyder et al. (1982) showed in a study of 20 different subjects that the mean total deposition for spontaneous breathing is virtually identical to that for controlled breathing at the same average flow rate. Heyder et al.'s data are given in Figure 10A-6, together with the values predicted for a reference male subject by the ICRP66 lung model. It is seen that, for both controlled and spontaneous mouth breathing, there is a large amount of variation

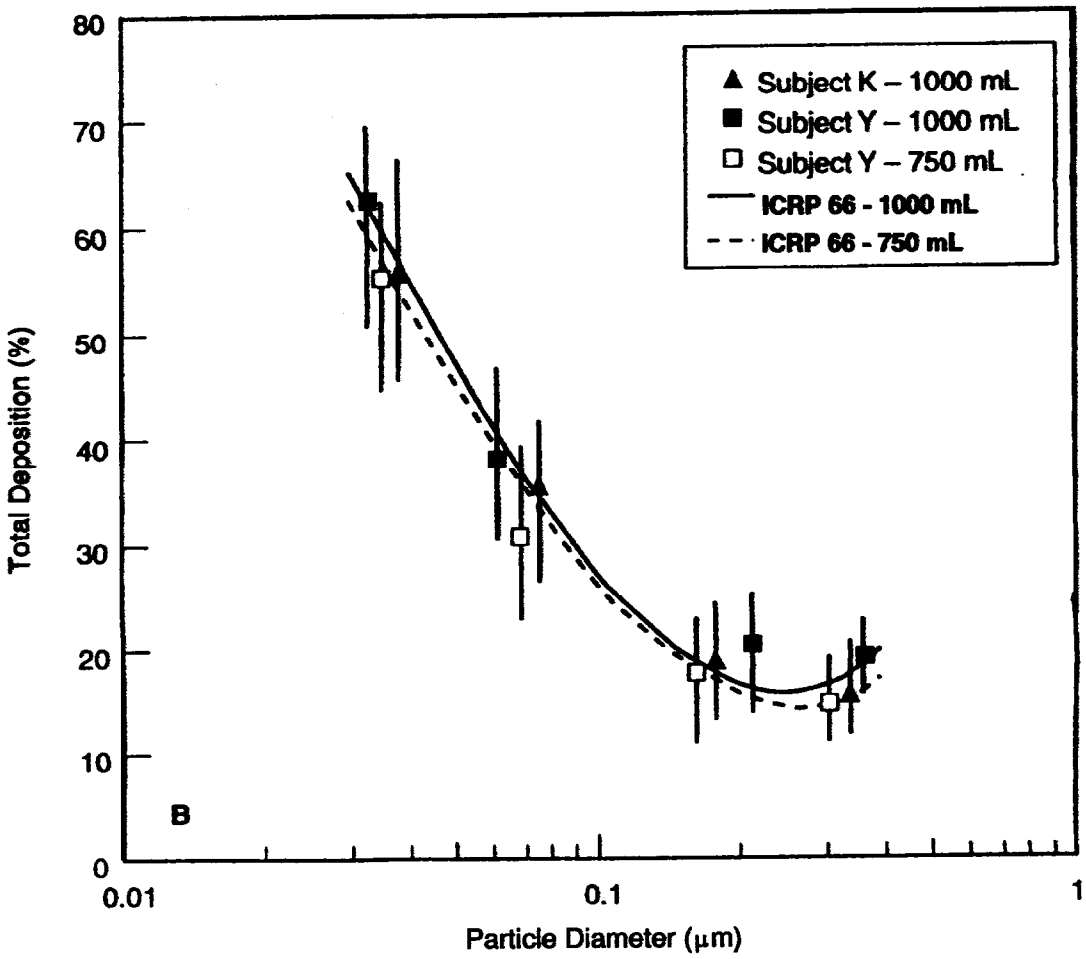

Figure 10A-5. Comparison of total respiratory tract deposition of submicron-sized alumino-silicate particles measured by Tu and Knutson (1984) in two subjects (at tidal volumes of 1000 mL or 750 mL), with the values calculated as a function of particle diameter by Egan et al. (1989). The ICRP Publication 66 (1994) lung model reproduces these calculated values.

Source: ICRP Publication 66 (1994).

between different subjects, although in any one subject under controlled breathing conditions, total deposition measurements are highly repeatable (Heyder et al., 1982).

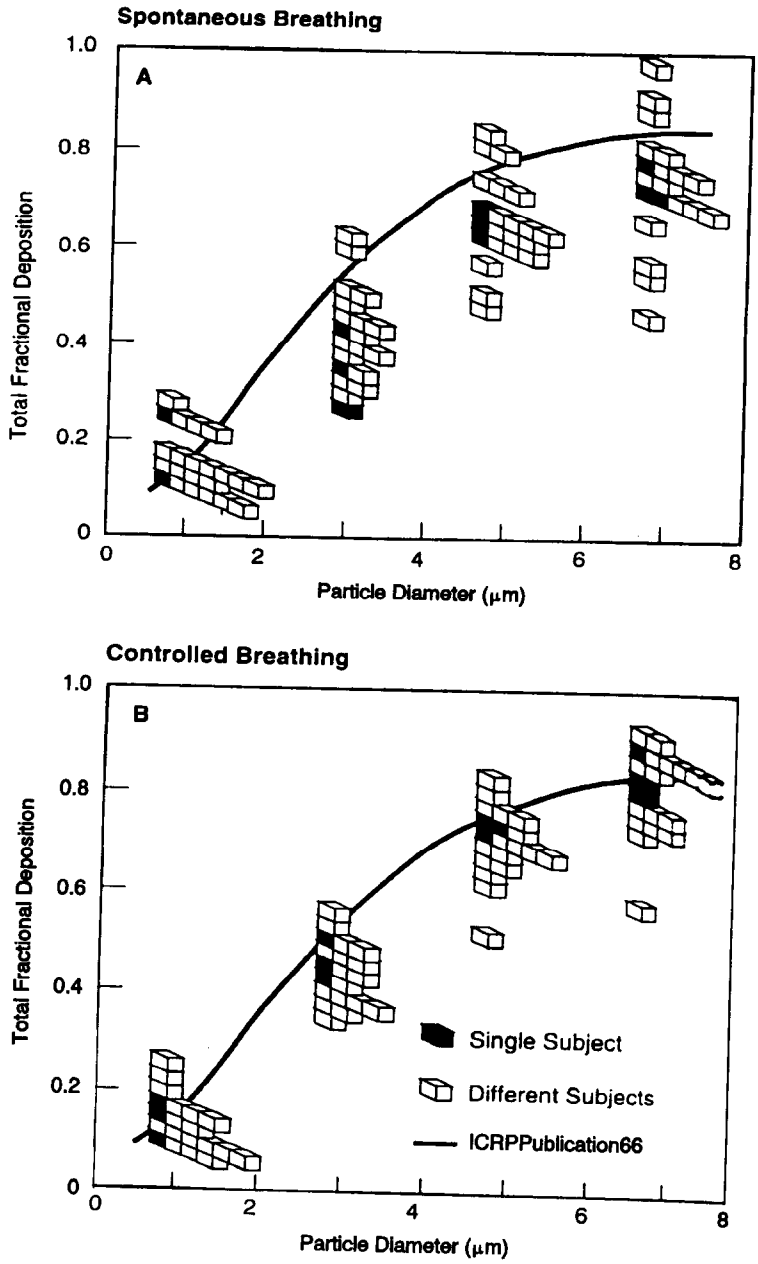

Figure 10A-6. Comparison of the distributions of total respiratory tract deposition measured in 20 different subjects (A) breathing spontaneously at rest or (B) breathing at a controlled rate at rest. In case (A), the individual mean flow rate varied from 220 to 740 mL/s, with a collective mean value of 380 mL/s. In case (B), the mean flow rate was held constant at 400 mL/s for each subject. Each box shown in the figure represents one experimental measurement. Shaded boxes represent repeat measurements on a single subject (see inset key in bottom figure). The curves show values predicted by the ICRP Publication 66 (1994) model.

Source: ICRP Publication 66 (1994).

10A.3.5 Comparison with Data for Iron Oxide Particles from New York University

Lippmann (1977) and Chan and Lippmann (1980) reported measurements of lung deposition and 24-h retention in a large number of different subjects at New York University (NYU). These studies involved iron oxide particles tagged in aqueous suspension with ^{99m}Tc (Wales et al., 1980). Each subject was allowed to breath normally, and the average tidal volume and breathing frequency were monitored. Typical values of these respiratory parameters were 500 cm^3 s^{-1} and 15 min^{-1}, respectively.

Figure 10A-7 shows the values of "fast-" and "slow-cleared" lung deposition obtained in these studies at NYU (adjusted from the measured value to zero extrathoracic deposition). In common with the earlier theoretical lung deposition models described by Yeh and Schum (1980) and Yu and Diu (1982b), and with the NCRP's currently proposed lung model, ICRP66's deposition model predicts substantially less bronchial ("fast-cleared") deposition for particles of aerodynamic diameter larger than 1 μm than is indicated by the bulk of the NYU data. Likewise, the predicted alveolar ("slow-cleared") deposition for particles of about 1-μm aerodynamic diameter is also low compared to the NYU data.

These data from NYU provide an excellent measure of intersubject variability in the deposition efficiencies of the tracheobronchiolar and alveolar-interstitial regions of the lungs. However, according to ICRP66's review of the literature, the interpretation of the NYU results is complicated by the possibility that the labeled iron oxide particles used may have grown hygroscopically in the humid air of the respiratory tract. Monodisperse iron oxide particles are produced by atomization of an aqueous suspension of colloidal iron oxide with a spinning top generator (Albert et al., 1964; Lippmann and Albert, 1967; Stahlhofen et al., 1979). The colloidal suspension is prepared by converting iron chloride in aqueous solution by hydrolysis to iron oxide. In order to remove all traces of the dissolvable chloride, the aqueous iron oxide colloid must be dialyzed extremely thoroughly.

Gebhart et al. (1988) used light-scattering photometry to examine the effect of the degree to which a suspension of colloidal iron oxide is dialyzed on the hygroscopicity of the resulting monodisperse particles, by comparing the physical properties of these particles on inhalation and exhalation. These authors found that even when the particles are produced from extremely well dialyzed iron oxide there is a distinct change in light-scattering

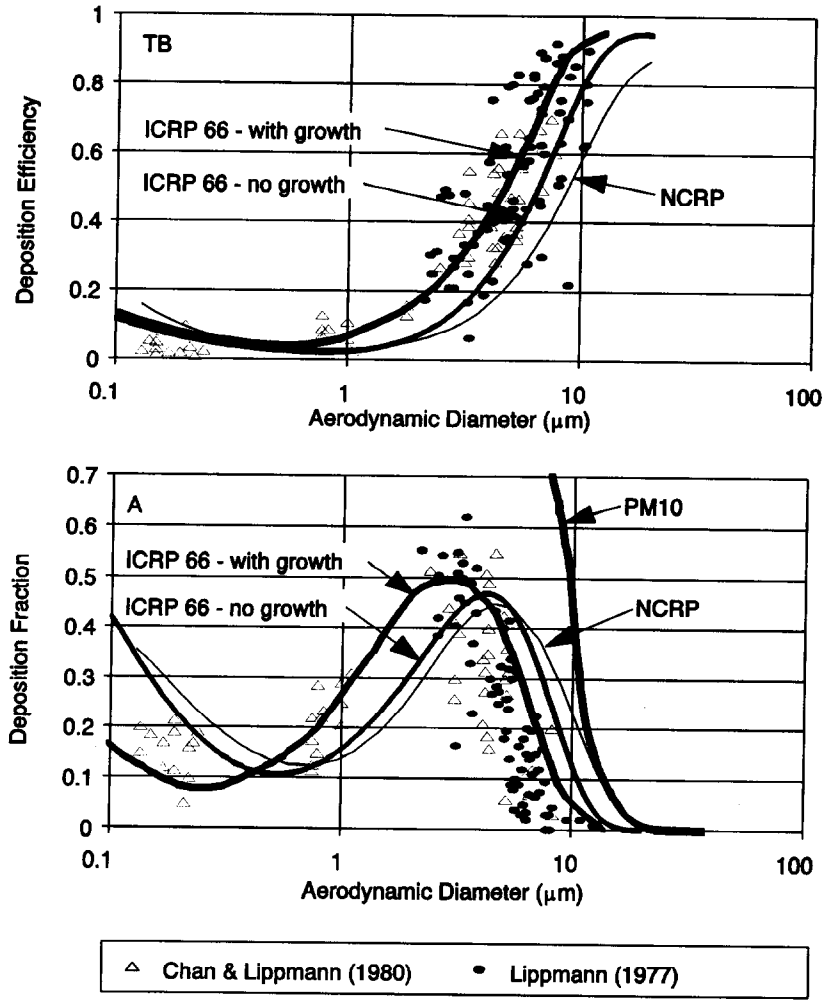

Figure 10A-7. Experimental data on deposition efficiency of the tracheobronchial (TB) region and fractional deposition in the alveolar (A) region for the large group of subjects studied at New York University (NYU). These subjects inhaled monodisperse particles of iron oxide through a mouthpiece at a tidal volume of approximately 1000 mL and respiratory frequency of 15/min. The measured values are normalized to zero extrathoracic deposition. The curves show the corresponding values predicted by the NCRP (proposed) and ICRP Publication 66 (1994) models. Two curves are shown for the ICRP 66 model: (1) "no growth" represents the values calculated on the assumption that the size of the iron oxide particles was stable in the respiratory tract, and (2) "with growth" represents the partial hygroscopic growth of similar particles indicated by the experimental study of Gebhart et al. (1988). The lower figure (marked as "A") also shows the characteristic particle collection efficiency curve for a PM_{10} sampler.

Source: Adapted from ICRP Publication 66 (1994).

properties between the inhaled and exhaled particles. Since the total respiratory tract deposition of these particles was indistinguishable from that of oil droplets of the same aerodynamic size in ambient air, Gebhart et al. (1988) concluded that their measured shift in optical properties was caused by the presence of a thin film of condensed water on the surface of the exhaled particles.

Using this same technique on a sample of the dialyzed iron oxide suspension prepared at NYU by their published method (Wales et al., 1980), Gebhart et al. (1988) found a much greater shift in light-scattering properties of the final monodisperse particles between inhalation and exhalation. This observed shift in light-scattering properties was accompanied by increased total respiratory tract deposition compared with that of oil droplets of the same aerodynamic size in ambient air. The deposition measured under identical exposure conditions was found to increase from 44% for the hydrophobic oil droplets to 68% for the iron oxide particles. The same change in measured respiratory tract deposition would be obtained by inhaling oil droplets of 3.8-μm aerodynamic diameter in place of the 2.4-μm-aerodynamic-diameter iron oxide particles.

The ICRP66 report includes a recommended method for extending the algebraic deposition model to evaluate regional lung deposition for aerosols that are subject to hygroscopic particle growth. Figure 10A-7 shows the effect on the modeled fast- and slow-cleared lung deposition including in the calculation the rate of hygroscopic growth of the NYU iron oxide particles that was derived from the results of the Gebhart et al. (1988) study. It is seen that this correction of the modeled lung deposition improves substantially the overall fit of the predicted values to the measurements.